

TEM-compatible microdevice for the complete thermoelectric characterization of epitaxially integrated Si-based nanowires

Supplementary Information

Jose M. Sojo-Gordillo,^{*,†,‡} Yashpreet Kaur,[‡] Saeko Tachikawa,^{¶,‡} Nerea Alayo,[†]
Marc Salleras,^{*,§} Nicolas Forrer,[‡] Luis Fonseca,^{*,§} Alex Morata,^{*,†} Albert
Tarancón,^{*,†,||} and Ilaria Zardo^{*,‡,⊥}

[†]*Catalonia Institute for Energy Research, IREC, Jardins de les Dones de Negre 1, 08930,
Sant Adrià de Besòs, Barcelona*

[‡]*University of Basel, Klingelbergstrasse 82, 4056, Basel, Switzerland*

[¶]*National Institute of Advanced Industrial Science and Technology, AIST, Tsukuba
1-1-1, Chuo Daisan Chuo Honkan 1F, Tsukuba, Japan*

[§]*Institute of Microelectronics of Barcelona, IMB-CNM (CSIC), C/Til·lers s/n, Campus
UAB, Bellaterra, 08193, Barcelona, Spain*

^{||}*ICREA, Passeig de Lluís Companys, 23, 08010 Barcelona, Spain*

[⊥]*Swiss Nanoscience Institute, SNI, Klingelbergstrasse 82, 4056, Basel, Switzerland*

E-mail: jose.sojo@unibas.ch; marc.salleras@imb-cnm.csic.es; luis.fonseca@imb-cnm.csic.es;
amorata@irec.cat; atarancon@irec.cat; ilaria.zardo@unibas.ch

Mechanical design and test

The deposition of Au nanoparticles used as NW seeds is a random process. Hence, after the device fabrication, it is likely that more than one pair of cantilevers get electrically connected by NWs. In order to increase the amount of successful samples where a single NW bridges one pair of cantilevers alone, the device is designed in such a way that the unwanted cantilevers can be mechanically disposed using micro-tips.

The mechanical specifications of the cantilevers were assessed with a Finite Element Method (FEM) simulation (see Figure S1). In the simulation, a perpendicular force emulating the pressing of micro-tip was applied at the center of the cantilever (circled area) ranging from 1 μN to 10 mN. Figure S1a shows one simulated case where the Von-Mises stress distribution is plotted for an applied force of 1 mN. Then, resulting maximum von Mises stresses – located at the narrowest part of the cantilever, i.e. the notches at its base – were compared with the maximum displacement expected at the adjacent cantilever as illustrates the inset of Figure S1b. Consequently, since the fail criteria for silicon is typically considered beyond a Von-Misses stress threshold of 500 MPa,²⁹ the expected deflection of the neighbor cantilever at failure can be estimated. Accordingly, the final dimensions of the cantilever was set so that the failure of the cantilever takes place with a maximum deflection of 10 nm at immediately adjacent cantilevers. In this way, if one would need to remove the adjacent cantilever where the NW of interest lays, the bending of the whole suspended platform will not damage the NW.

Mechanical removal of undesired cantilevers was verified using micro-tips as depicts Figure S1c. It can be observed how their disposal does not damage neighbor positions, as designed. In this way, the mechanical design of the notches patterned at the cantilever base described in subsection 3.1 is experimentally validated.

Raman thermometry calibration

Figure S2 depicts the results of the calibration process of the Raman shift as a function of temperature ($\partial\omega_0/\partial T$) using both laser (Figure S2a) and Joule heating (Figure S2). In both cases, the shift in the Stokes Raman peak was probed at the central position of the NW, the most sensitive

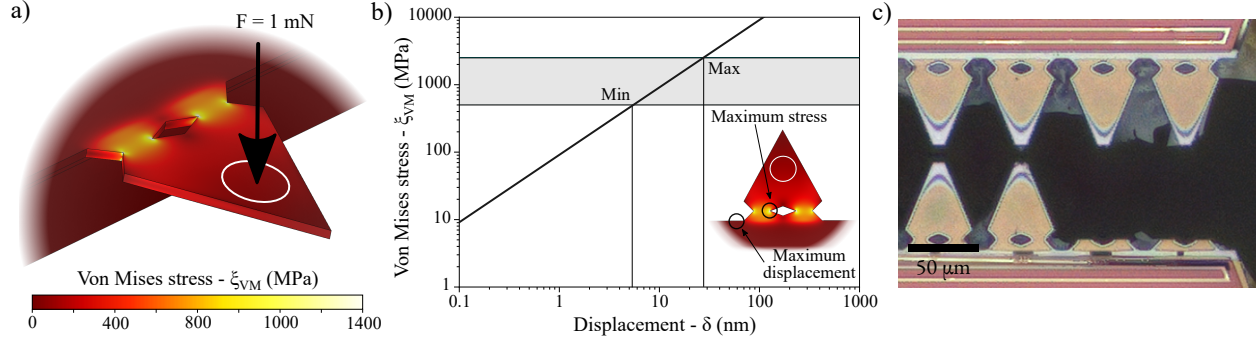


Figure S1: a) FEM mechanical simulation of a cantilever upon the application of a 1 mN force over the circled area. The color scale represents the calculated von Mises stress. b) Resulting maximum von Mises stress as a function of the maximum displacement measured at the adjacent cantilever position as illustrated in the inset. The grey area illustrates the range where silicon fracture happens.²⁹ c) Confocal image of the cantilever after the controlled removal of the rightmost bottom cantilevers. No damage was caused to adjacent cantilevers.

to changes in temperature.^{27,43} This laser spot position corresponds to the fifth (middle) optical image of Figure 7b. Hence, the ordinate at the origin (ω_0) for both studies yields the virtual peak position at the substrate temperature used while no heating takes place, i.e. when $P_{Laser} \rightarrow 0$. The temperature dependence of the NW Raman peak in this negligible heating limit ($\partial\omega_0/\partial T$) was fitted in the inset of Figure S2a. This calibration is used to translate a relative Raman shift into a temperature increase (see Figure 7a). Finally, the inset of Figure S2b shows two example of spectra acquired while applying (or not) Joule heating.

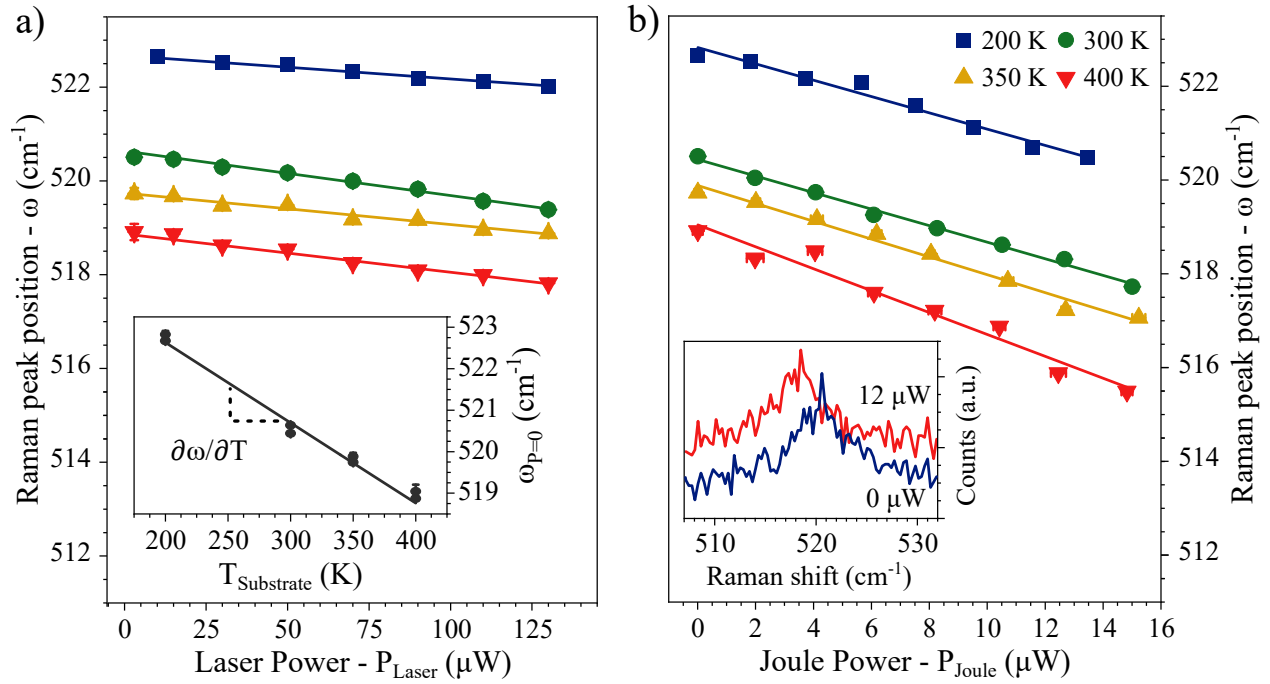


Figure S2: a) Raman peak position as a function of the laser power (measured before the objective) for the same temperature range. The inset shows the resulting fitted Raman peak position with null power ω_0 at the ranged temperatures. The solid line represents the linear fit of the data. b) Raman peak position as a function of the applied Joule power through the NW for substrate temperatures ranging from 200 to 400 K. The inset shows a comparison between the acquired spectra at $T_{\text{Substrate}} = 300\text{ K}$ with null (blue) and 12 μW (red) Joule power applied.